excitation level, it is closely approached at 10 mph as expected. At higher speeds the value of ζ_1 is lower and the limit point of stability will correspond to a lower value of ζ_2, and, hence, a lower limit on the g-level. This is clearly demonstrated by the decreasing trend in g-level both with and without damper application.

Further testing is still underway which will help trace the lower boundaries of the stability loop as x changes with progressive brake wear. In this case it is still necessary to repeat the test without the damper to make sure that the excitation level has not changed or to make necessary adjustments in the applicable value of ζ_1.

VIII. Conclusions

The problem of the self-excited two-mass system has been analyzed and a closed-form solution obtained. The conditions of stability of either or both modes have been discussed thoroughly. An outline of the nature of brake excitation is given. Energy method is utilized to treat the possible nonlinear functions introduced in the system. It has been shown that a self-excited two-mass system possesses the property of being stable within a defined range of frequency ratio and secondary system damping. The range of stability is affected by the mass ratio and the negative damping in the system. Reference has been made to the problem when defined by a brake fitted with a tuned damper. The stability charts can then serve as design charts capable of indicating the optimum size, tuning, and damping to be accommodated in a secondary system intended as a damper for a primary brake system. The problem of damping the secondary system by hydraulic (velocity-square damping) rather than viscous means is discussed and the method of utilizing the stability charts outlined. It has been shown that with hydraulic damping the margin of stability is increased but some limiting oscillations of predetermined value have to be allowed within the system. Viscous damping has a smaller range of stability but should damp out any vibration completely; the limiting value in this case is zero amplitude.

The experimental results have confirmed the validity of the theoretical analysis to predict the brake response when fitted with a tuned damper. The brake vibrations were suppressed successfully within the design limits of the damper. The success of this application, without adding an appreciable weight to the brake, represents a long-sought method for control of vibration in brakes. It opens the door for utilizing the harder, more economical linings with the subsequent savings on weight and service cost and increased lining life.

References

[1] Black, R. J., "Evaluation of Brake Lining Materials from Vibration Standpoint, Chatter Tester to Airplane Correlation Methods," Rept. ECD-WV-60-1, unpublished, The Bendix Corp.

[2] Abu-Akeel, A. K., "An Analytical Approach to the Study of Tuned Damper Application to Brake Vibrations," Rept. ECD-WV-67-5, The Bendix Corp.

JAN.-FEB. 1969 J. AIRCRAFT VOL. 6, NO. 1

Jet-Pump Actuation of Variable-Density Subsonic Wind Tunnels

J. C. Gibbings*
University of Liverpool, Liverpool, England

The actuation by jet pumps of variable-density, closed-circuit, subsonic wind tunnels is compared with an existing one-dimensional analysis. The measured performance is correlated in terms of the wind-tunnel power factor. The off-design characteristics of the outlet jet pump under suction conditions are studied, and its performance in combination with the actuator jet pump is given. Two methods of intermittent operation from a storage reservoir are compared.

Nomenclature

a^* = speed of sound for $M = 1$
A = const, Appendix A
A = (with subscript) cross-sectional area
B = const, Appendix A
C = const, Appendix A
C_1,C_2,C_3 = consts, Appendix A
C_f = friction coefficient
C_p = coefficient of specific heat at constant pressure
D = diameter of mixing length
h = specific enthalpy
K = const, Appendix A
L = length of mixing length
m = (with subscript) rate of mass flow
M = (with subscript) Mach number
p = (with subscript) pressure
P = tunnel power factor
R = gas constant
Re = Reynolds number
S = surface area of mixing length
t = tunnel running time
T = (with subscript) temperature
v = (with subscript) velocity
V = reservoir volume
α = const, Appendix A
β = area ratio A_3''/A_3', Appendix A
γ = ratio of the specific heats
η = diffuser efficiency
μ = (with subscripts) mass-flow ratio, secondary to primary flow
ρ = (with subscripts) density
σ = tunnel pressure ratio
ϕ = velocity ratio, Appendix A
ϕ = (with subscripts) nozzle loss coefficient
ϕ_n = friction coefficient, Appendix A
ψ = density ratio, Appendix A

Subscripts

0 = actuator outlet stagnation conditions; also outlet jet pump

Received January 8, 1968; revision received July 22, 1968.

* Lecturer, Department of Mechanical Engineering, Fluid Mechanics Division.

1,2,3, 4,5 = pertaining to stations in Fig. 1
41, 42 = pertaining to the two roots of the jet-pump equations
4_s = stagnation value at station 4
a = actuator jet pump
atm = atmospheric
i = actuator inlet stagnation condition
R = reservoir conditions
R_f = final reservoir conditions
R_0 = initial reservoir conditions
T = total air supply
w = tunnel working section conditions

1. Introduction

THE large capital and running costs of high-speed wind tunnels that are actuated continuously by fans have given impetus to the development of intermittent operation. There are two forms of operation for intermittently running wind tunnels. In one, all the air passing through the test section flows between two air reservoirs that are initially at different pressures and one of which may be the atmosphere. The other form makes use of a jet pump whose primary flow is from a high-pressure supply and whose secondary induced flow is that through the wind tunnel.

Pioneer experimental work on jet-pump tunnels operated by compressed air was done by Bailey and Wood[1] and by Stack.[2] Further work has been described by Bailey and Wood both for subsonic tunnels[3,4] and for supersonic tunnels,[5] and further extensive development has been reviewed by Knowler and Holder.[6] Experimental investigations on the use of steam as the actuating fluid have been made by Poggi[7] and by Lilley and Holder.[8] The first performance analysis of a jet-pump tunnel appears to have been given by Winter,[9] who compared his solutions with experimental results.

Use of a closed-circuit wind tunnel permits a variation of the pressure in the test section, thus enabling an independent control of the Reynolds number and of the Mach Number.

Such a tunnel is shown diagramatically in Fig. 1. In this arrangement, the flow around the tunnel circuit is maintained by the actuator jet pump, whose high-velocity primary flow is fed through an annular nozzle. A mass flow rate of air which is equivalent to the rate through this annular nozzle is removed by the outlet jet pump, which is needed only when the air pressure in the tunnel return circuit is below atmospheric pressure. By this arrangement, only the high-pressure air supply to the actuator jet pump needs to be dried, thus affecting economies in the drying plant.†

Both operation at a low air density and the lower power factor associated with return circuit tunnels decrease power requirements. The existence of such effects are here investigated for a jet-pump drive.

Throttling of the air at outlet from the tunnel circuit will raise the tunnel air density, whereas use of the outlet jet pump will decrease it. These methods of control are to be discussed.

2. Analysis of the Jet Pump

A paper by Keenan and Neuman[10] has shown that a one-dimensional analysis can give good performance predictions for a jet pump with a central convergent-divergent nozzle and a parallel mixing length discharging to outlet. A paper by Winter[9] has also shown good agreement between this theory and experiment using an annular nozzle, a parallel mixing length, and a conical diffuser. Both these papers presented computed results for which frictional losses on the walls were excluded, except that Winter allowed for the diffuser loss. However, for the different range of operating conditions considered here, neglect of this friction has, as was observed by Keenan, Neumann, and Lustwerk,[11] a large effect on the optimum predicted performance. In Flugel's presentation of the theory, inclusion of empirical coefficients accounted for these frictional losses.[12]

Referring to the sketch of a jet pump in Fig. 2, it is found that the theory gives two solutions for conditions at station 4 after mixing in a constant cross-sectional area between stations 3 and 4. Winter pointed out[9] that the two roots of the equation give velocities v_{41} and v_{42} that are related by $v_{41} \cdot v_{42} = a^{*2}$, which is the relation for a normal shock wave. Keenan, Neumann, and Lustwerk[11] have obtained, for a jet pump with a central primary nozzle, experimental conditions appropriate to both the subsonic and the supersonic roots. Both these conditions have been observed also during experiments on a jet pump with an annular nozzle.[13] For the supersonic root the shock has either to be passed into a supersonic diffuser[14] or swallowed into a subsonic diffuser, in which latter case, unless the shock was quite weak, the over-all loss would be greater than with the subsonic root. With an annular nozzle in which mixing takes place in a conical diffuser, as in the present configuration of the tunnel actuator jet pump, conditions after mixing seem always to correspond to a subsonic Mach number.[15]

3. Numerical Solutions for the Outlet Jet Pump

Most of the published studies of jet pumps are concerned with operation at the design conditions. The present application to pumping the tunnel outlet flow would most conveniently require the operation of a jet pump of largely fixed shape over a range of conditions, and so the off-design characteristics are now considered.

Using the one-dimensional equations governing the jet-pump flow (Appendix 1) and with subscripts to denote the stations numbered in Fig. 2, calculations were performed for the following loss coefficients suggested by Flugel[12] and a diffuser efficiency as defined by Liepmann and Puckett[16]

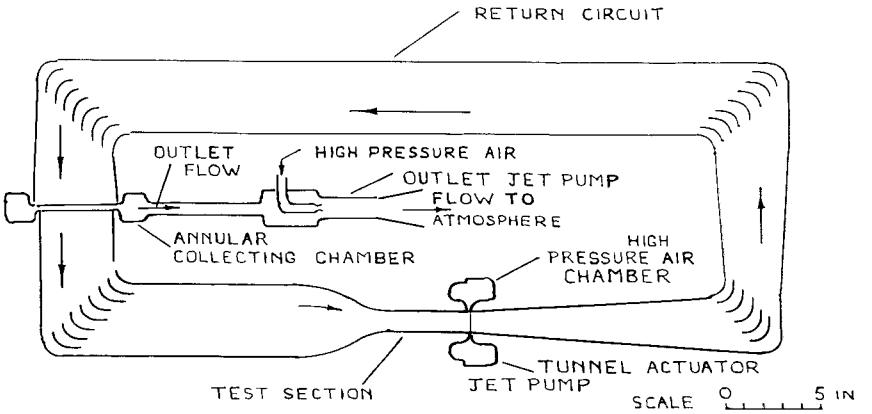

Fig. 1 Diagram of the closed-circuit wind tunnel showing the actuator jet pump to drive the tunnel flow and the outlet jet pump to remove air from the circuit. (Note: the outlet jet pump is not drawn to scale.)

† The necessity for a dry airstream in the working section precludes the use of steam as an actuating fluid in a closed-circuit tunnel.

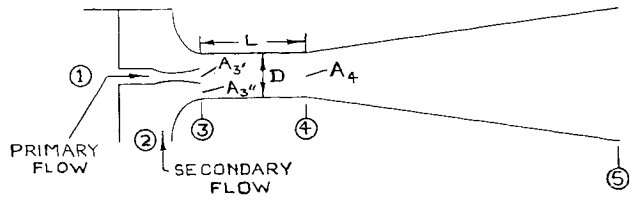

Fig. 2 Diagram of the outlet jet pump. (Note: stations 1, 2, and 5 are at stagnation conditions.)

primary nozzle loss coefficient $\phi_1^2 = 0.95$, secondary nozzle loss coefficient $\phi_2^2 = 0.85$, mixing-length friction coefficient $C_f = 0.004$, and diffuser efficiency $\eta = 0.75$.

Computations were performed for the stagnation temperatures $T_1 = T_2 = 288°K$ and for the four cases; case A, $p_1/p_2 = 8.84$, $p_2/p_5 = 0.5$; case B, $p_1/p_2 = 15.63$, $p_2/p_5 = 0.5$; case C, $p_1/p_2 = 8.84$, $p_2/p_5 = 0.5$, $\phi_1 = \phi_2 = 1.0$; and Case D, $p_1/p_2 = 8.84$, $p_2/p_5 = 0.75$. The results obtained are illustrated by the correspondingly lettered curves in Figs. 3 and 4. Figure 3 is a plot of the ratio μ of the secondary mass-flow rate to the primary mass-flow rate against the Mach number M_3'' of the secondary flow at the entrance to the mixing tube. Figure 4 is a plot of μ against the ratio β, which is the ratio of areas A_3''/A_3' at entrance to the mixing tube.

All four curves of Fig. 3 exhibit the maxima that have been observed by Keenan, Neumann, and Lustwerk[11] and an approximate analysis for which has been given by Elrod.[17]‡ Two features common to all four curves are of interest. First, the mass-flow ratio does not drop rapidly either side of the maximum value, and second, the Mach number of the induced flow at this maximum is fairly high in the region of 0.6 to 0.85.

Comparison of curves A and B shows that roughly doubling the actuating pressure increases the maximum value of μ by only 26%, the optimum Mach number remaining almost unchanged. In marked contrast, comparison of curves A and C shows that neglecting friction in the primary and secondary nozzles raises the mass-flow ratio by 30% and the optimum Mach number to about 0.9. Finally, curve D in

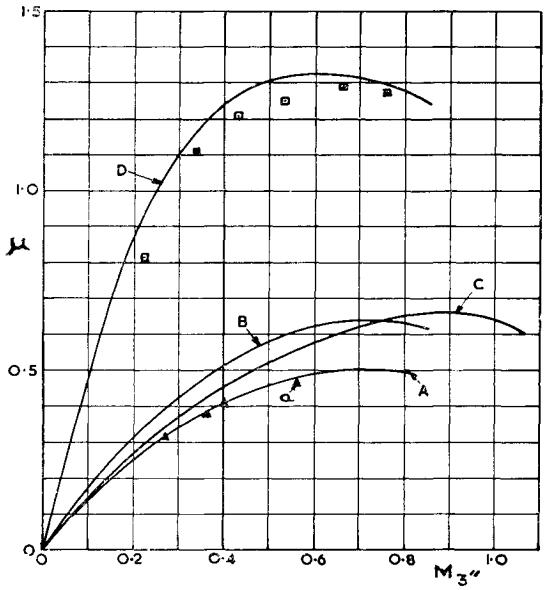

Fig. 3 Variation of the mass-flow ratio μ as a function of the Mach number of the secondary flow at entrance to the mixing tube for four cases detailed in the text.

‡ The approximations of Elrod's analysis are not valid for these examples.

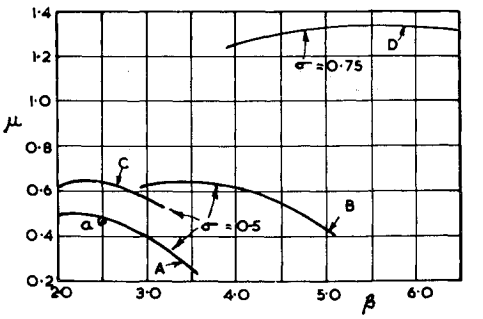

Fig. 4 Variations of the mass-flow ratio μ as a function of the ratio of the secondary to primary flow cross-sectional areas β.

comparison with curve A shows that the smaller pressure rise across the jet pump results in a marked increase in μ.

The corresponding plots in Fig. 4, of mass-flow ratio against area ratio, also show curves with gentle variations of gradient in the region of the maxima. Here, the effect of friction in the nozzles is shown, by comparison of curves A and C, to have little effect upon the optimum value of β.

4. Numerical Solutions for the Tunnel Actuator Jet Pump

Calculations of the power requirements of wind tunnels commonly are based upon an estimation of the power factor P, which accounts for all losses except that represented by the fan or compressor efficiency.[18] It is written,

$$P \equiv \frac{\text{Rate of work input to the tunnel stream}}{\text{Rate of flow of kinetic energy at the working section}}$$

and is usually estimated largely from empirical data.[19,20]

As a wind-tunnel power unit consists of a compressor and a cooler, and as a jet pump is representative of this combination, then

$$P = C_p T_i[(p_0/p_i)^{(\gamma-1)/\gamma} - 1]/(\tfrac{1}{2}v_w^2) \qquad (1)$$

where T_i and p_i are, respectively, the stagnation temperature and stagnation pressure at inlet to the actuator, p_0 is the outlet stagnation pressure, and v_w is the velocity in the working section.

Noting that the tunnel Mach number M_w is given by

$$M_w^2 = v_w^2/[(\gamma - 1)C_p T_w]$$

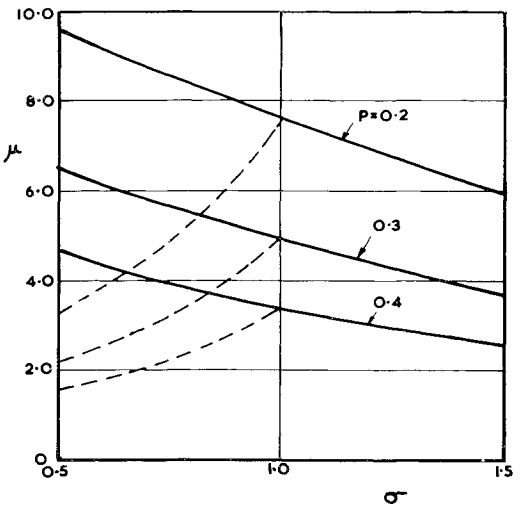

Fig. 5 Variation of the mass flow ratio μ for the actuator jet pump as a function of the tunnel pressure ratio σ and for three values of the tunnel power factor P. Dotted lines for combined operation with the outlet jet pump.

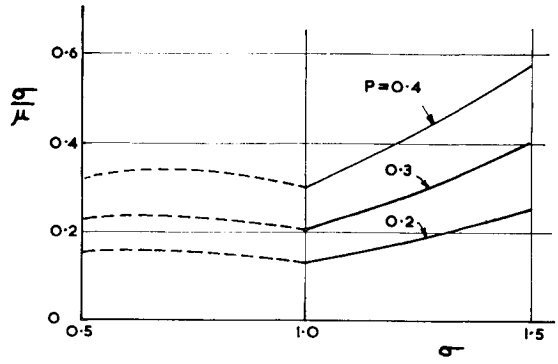

Fig. 6 Variation of the total high-pressure air-consumption parameter σ/μ as a function of the tunnel pressure ratio σ and for three values of the tunnel power factor P.

and that

$$T_i/T_w = 1 + [(\gamma - 1)/2]M_w^2$$

then,

$$P = \frac{1 + [(\gamma - 1)/2]M_w^2}{[(\gamma - 1)/2]M_w^2}\left[\left(\frac{p_0}{p_i}\right)^{(\gamma-1)/\gamma} - 1\right] \quad (2)$$

When the actuator is situated immediately at the end of the working section then, introducing the jet-pump notation illustrated in Fig. 2, $M_w = M_3''$, $p_i = p_{3s}''$, and $p_0 = p_{4s}$, where the subscript s indicates a stagnation value.

A numerical example was computed for $p_1/p_{atm} = 4.42$, $T_1 = T_2 = 288°\text{K}$, $\phi_1^2 = 0.95$, $M_w = M_3'' = 0.9$ and where the tunnel pressure ratio σ is given by $\sigma = p_{3s}''/p_{\text{atm}}$. Results of the calculation are shown in Fig. 5 as the solid lines in a plot of the mass-flow ratio μ against σ for three values of P. A marked increase in μ is seen to result from a reduction in either P or σ.

5. Numerical Solutions for the Tunnel Performance

When the tunnel stagnation pressure p_{3s}'' is less than atmospheric so that $\sigma < 1.0$, the outlet and actuator jet pumps operate simultaneously. Indicating their mass-flow ratios by μ_0 and μ_a, respectively, and noting that the rate of flow of the actuator primary jet and the outlet secondary stream are equal, then the ratio μ_T of the mass-flow rate through the tunnel test section to the sum of the high-pressure mass-flow rates to both jet pumps is given by

$$\mu_T = (\mu_a\mu_0)/(1 + \mu_0) \quad (3)$$

For the outlet jet pump, A_3'' will usually be fixed, but the Mach number M_3'' will vary with variation in the primary flow rate of the actuator. However, the flatness of the peaks of the curves of Fig. 3 means, for the present example, that this off-design condition does not involve a large performance penalty.[21] Using the maximum values of curves A and D in Fig. 3, computed values of μ_T are plotted in Fig. 5 as dotted lines.

It is seen that the total mass-flow ratio decreases considerably as σ decreases below 1.0. Increasing the primary air pressure of the outlet jet pump corresponding to curve B of Fig. 3 increased μ_0 by 26%, but from Eq. (3) this only increases μ_T by 16%. In contrast, use of Winter's results[9] shows that a corresponding increase in the actuator primary air pressure gives an increase of 50% in μ_a and hence from Eq. (3) gives the same increase in μ_T.

For a test section cross-sectional area A_w the total air consumption rate m_T is

$$m_T \propto (A_w\sigma)/\mu_T \quad (4)$$

and so the total high-pressure air consumption is proportional

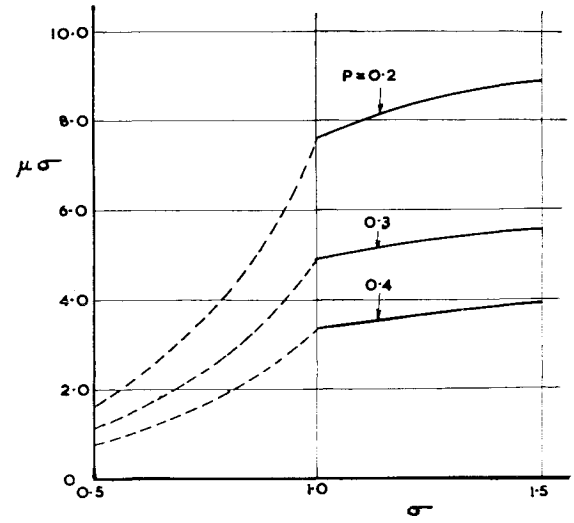

Fig. 7 Variation of the design criterion $\mu\sigma$ as a function of the tunnel pressure ratio σ and for three values of the tunnel power factor P.

to σ/μ_T. Values are shown plotted in Fig. 6. A steep rise in air consumption is seen to result from an increase in σ above the value of 1.0. Under suction conditions the consumption for this example is almost constant with change in σ.

The Reynolds number of the flow in the tunnel test section, Re, is

$$Re \propto \sigma A_w^{1/2} \quad (5)$$

and substitution from Eq. (4) gives

$$Re^2/m_T \propto \mu_T\sigma$$

Values of this design criterion are shown plotted in Fig. 7. The results show that for a fixed Reynolds number the air consumption falls with increase in σ with, from Eq. (5), a corresponding decrease in A_w.

Control of a jet-pump tunnel to maintain constant tunnel speed while operated from a storage reservoir can be affected during the fall in reservoir pressure, by either throttling the air supply so as to supply it to the actuator nozzle at a constant pressure or by varying the area of the actuator nozzle.[21,6] A comparison of these two methods was made using the computed results given by Winter[9] for a tunnel power factor of 0.25 and a frictionless primary flow in the actuator nozzle driving the tunnel at $M_w = 1.0$ for $\sigma = 1.0$.

Using the standard relations[22] quoted in Appendix B, the tunnel running time t, for the flow throttled to a constant pressure from an initial reservoir pressure p_{R0} of 25 p_{atm}, is shown in nondimensional form as curve A in Fig. 8. The variation of temperature T_1 during the running down of the reservoir pressure was found to have a negligible effect,[21] and so has been neglected in this example. It is seen from

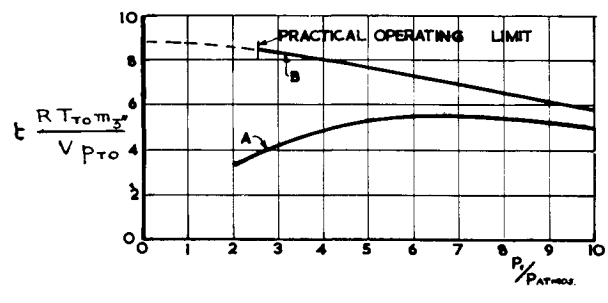

Fig. 8 Tunnel running time with air supply from a storage tank. Case A, throttling of air to actuator jet-pump nozzle; case B, adjustable nozzle on actuator jet pump.

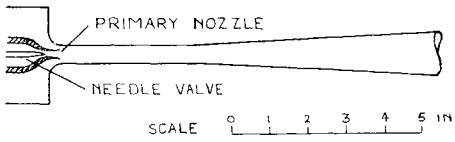

Fig. 9 Scale diagram of outlet jet pump.

Fig. 8 that the running time has a maximum for an operating pressure of 6.3 p_{atm}, the variation either side of this maximum being a gentle one.

Using the relation derived in Appendix B, the running time for the variable nozzle method of control was computed and results are shown as curve B in Fig. 8. The lowest value to which the reservoir pressure could be expanded would in practice be limited by mechanical features of an adjustable nozzle. A value of 2.5 p_{atm} is indicated in Fig. 8 and is based on experience obtained during the experimental work described later. It is seen that there is little advantage in making this limit much lower. Comparison of curves A and B shows the considerable increase of 53% in the running time by using the variable nozzle method.

6. Experimental Measurements

Experiments were performed on a model wind tunnel, a sketch of which is shown in Fig. 1. The outlet jet pump is shown sketched to scale in Fig. 9 and the annular nozzle is shown in outline in Fig. 10. Further details are given in Ref. 21.

The experiments upon the outlet jet pump aimed at investigating the effects of operating at other than design conditions. With the needle valve fully open in the outlet jet pump primary nozzle (Fig. 9) the mass-flow rate measured by an orifice meter corresponded to a friction coefficient ϕ_1^2 of 0.95. This is the value used in the numerical work presented in Sec. 3.

Results of the measurements of mass-flow ratio are given as the experimental points in Fig. 3. In view of the large effects of friction already discussed, together with the use of estimated frictional coefficients, the agreement of the experiments with curves A and D for $\sigma = 0.5$ and 0.75, respectively, is satisfactory.

This outlet jet pump was designed, with the needle valve fully open, to operate at the following conditions. Nozzle outlet area: throat area = 2.12:1, $M_3'' = 0.577$, $\beta = 2.48$. The corresponding experimental point marked 'a' in Figs. 3 and 4 is seen to give good agreement with these design conditions. All the other experimental points both for $\sigma = 0.5$ and $\sigma = 0.75$ were obtained with the needle valve in partially closed positions, and it is seen that equally good agreement with the calculated values is obtained for these off-design conditions when the independent variable is M_3''.

Experiments upon the actuator jet pump gave results of which Fig. 11 presents a typical example for the variation of

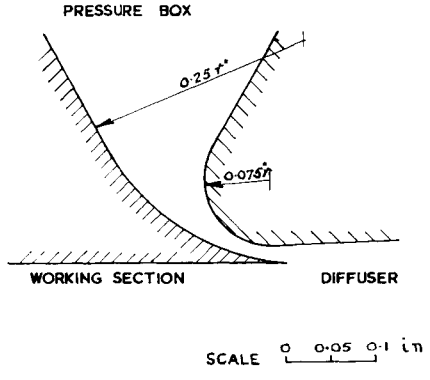

Fig. 10 Scale diagram of annular nozzle of actuator jet pump.

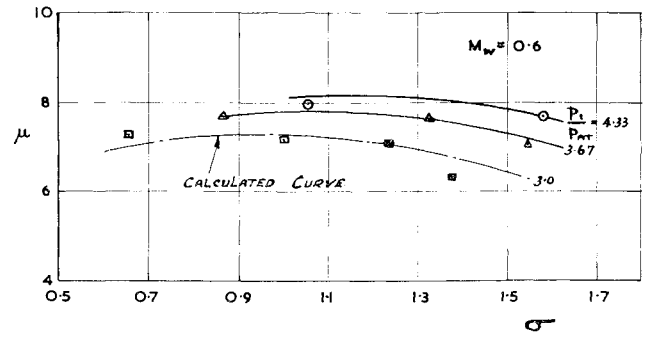

Fig. 11 Measured values of the mass flow ratio μ as a function of the tunnel pressure ratio σ for three values of the pressure of the air supply to the jet pumps.

the mass-flow ratio with the pressure ratio. Comparison with Fig. 5 shows a marked difference in the nature of the curves, a point returned to later.

The product of the pressure ratio σ and the velocity in the tunnel settling length upstream of the contraction can be used as a measure of the Reynolds number of the flow around the circuit. The tunnel power factor P would be expected to be a function of this Reynolds number.

All the experimental results were used to compute values of P, the measured value of the Mach number in the plane of the actuator nozzle being identified with M_3''. The jet-pump performance analysis of Appendix A assumes the existence of a parallel mixing length. Winter's experimental work[9] seems to indicate that, when the nozzle is an annular one feeding directly into the entrance to a conical diffuser as in the present apparatus, the results agree well with this analysis. He further found that the addition of a parallel mixing length impaired the performance through the addition of the added wall friction. Reid[15] has further shown that the annular jet without the parallel mixing length suppresses the diffuser separation. However, it is known[12] that with a central jet, as in the outlet jet pump, a parallel mixing length is necessary.

The values of σ were multiplied in the proportion of the velocity in the settling length to that when $M_w = 0.6$. The results are seen in Fig. 12. They all fall around one mean line, thus supporting the idea that the performance of a subsonic jet-pump wind tunnel can be based on the usual tunnel power factor.

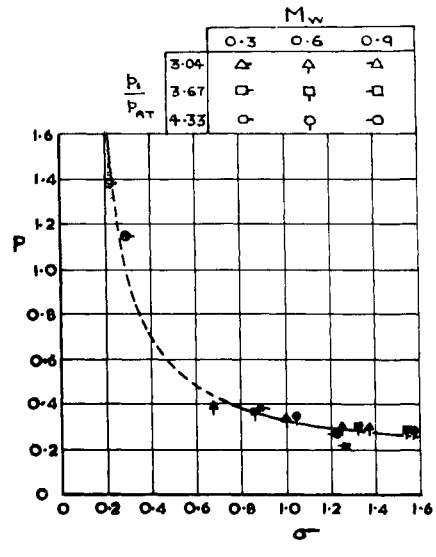

Fig. 12 Deduced values of the tunnel power factor as a function of the tunnel pressure ratio used as a scale of tunnel Reynolds number.

Because of a slight design underestimation of the boundary-layer growth along the walls of the working section, when $M_w = 0.9$ the Mach number dropped to $M_3'' = 0.84$ in the plane of the actuator nozzle. In one case the measured value of the mass-flow ratio was $\mu = 6.0$, giving a computed value of $P = 0.27$. If M_3'' had been 0.9 then for this power factor the mass-flow ratio would have dropped to a computed value of 5.6. The Mach number drop along the working section meant that the actuator jet pump was working nearer to an optimum condition of the form illustrated for the outlet jet pump in Fig. 2.

There is evidence in Fig. 12 of a large-scale effect upon the power factor. In this type of tunnel and at this scale, most of the losses occur through the corner vanes. Collar has performed experiments upon the Reynolds number effect on thin plate vanes, as used here.[23] Analyzing his results shows that the loss is proportional to $Re^{-0.62}$. A curve representing

$$P \propto \sigma^{-0.62} \tag{6}$$

is drawn as a solid line in Fig. 12 down to the point corresponding to a vane Reynolds number of 5.10^4, which was the lower limit of Collar's experiments. It is seen to explain satisfactorily the variation of P with σ. At a lower Reynolds number the corresponding index of Eq. (6) becomes more negative in accordance with common experience for friction losses. The dotted curve of Fig. 12 is drawn for an index of -0.8.

This variation of P has the marked effect upon mass-flow ratios already observed. This is illustrated by the chain curve of Fig. 11, which has been computed to satisfy Eq. (6). This curve is seen to fit the experimental values and now explains the difference from the type of curves of Fig. 5.

Operating the actuator nozzle at pressure ratios higher than the design values results in the primary jet expanding on outlet, and hence contracting the secondary stream before appreciable mixing can take place. Bailey and Wood[1] observed that this could result in choking of the secondary flow. Four such instances of sonic speed downstream of the plane of the annular nozzle were observed with the present tunnel by traverse of a static tube along the centerline of the tunnel duct.

The measured conditions are tabulated in the first four lines of Table 1. The measured flow characteristics of the actuator nozzle corresponded to $\phi_1^2 = 0.95$. Using this value and knowing the nozzle shape, p_3' was calculated and is given in the fifth row of Table 1 as a ratio of p_3''. Increase in this ratio increases the expansion of the jet at outlet from the nozzle[24,25] and hence, as is shown in this table, reduces the area of the secondary stream and consequently, under choking conditions, also the working-section Mach number.

The final line in this table gives the calculated values of M_3'' using the isentropic flow analysis given by Lindsey.[26] The agreement with the measured values is reasonable, the effect of friction being to underestimate the reduction in tunnel Mach number due to choking.

Table 1 (Measured and calculated tunnel) Mach numbers for the condition of choking of the tunnel flow at the actuator jet pump

M_w	0.885	0.825	0.81	0.752
σ	1.00	1.39	1.07	1.12
M_3'' (measured)	0.80	0.78	0.77	0.72
p_1/p_2	4.41	3.17	3.49	3.93
p_3'/p_3''	1.71	1.20	2.58	2.78
M_3'' (calculated)	0.82	0.83	0.80	0.79

Appendix A: Jet-Pump Equations

The friction in either the primary or the secondary nozzles is accounted for by writing the momentum equation in the form

$$dp/\rho + (v/\phi_n^2)dv = 0$$

where ϕ_n is the friction coefficient. The corresponding relations for the one-dimensional flow then follow readily.[25]

Friction in the mixing tube is accounted for by writing the frictional force as $C_f \frac{1}{2}\rho v^2 S$ where the surface area S is given by

$$S = (4L/D)(A_3' + A_3'')$$

In the numerical examples it was found that $\rho_3'' v_3''^2$ was roughly the same as $\rho_4 v_4^2$.

Following Winter by writing[9]

$$\phi \equiv v_3'/v_3'' \qquad \psi \equiv \rho_3'/\rho_3''$$

$$\beta \equiv A_3''/A_3'$$

$$\alpha \equiv p_3/(\rho_3'' v_3''^2) = 1/(\gamma M_3''^2)$$

$$K \equiv 1 + (2C_f L/D) \qquad \mu \equiv m_3''/m_3'$$

the mixing equations can be written

$$v_4\rho_4 = \rho_3'' v_3''[(\phi\psi + \beta)/(\beta + 1)] \equiv C_1$$

$$p_4 + K\rho_4 v_4^2 = \rho_3'' v_3''^2[\alpha + (\phi^2\psi + \beta)/(\beta + 1)] \equiv C_2$$

$$\gamma/(\gamma - 1)(p_4/\rho_4) + \tfrac{1}{2}v_4^2 = (\phi\psi h_1 + \beta h_2)/(\theta\psi + \beta) \equiv C_3$$

Solutions for the properties after mixing are quadratic in form. For the velocity,

$$v_4 = \frac{C_2/C_1 \pm \{(C_2/C_1)^2 - 4[K - (\gamma - 1)/2\gamma] \times (\gamma - 1)C_3/\gamma\}^{1/2}}{2K - (\gamma - 1)/\gamma}$$

Alternatively Weatherston's Mach number functions can be used.[27] When the pressure after mixing is specified a cubic in β is obtainable. When additionally $T_1 = T_2$, this reduces to the quadratic

$$A\beta^2 + B\beta + C = 0$$

where

$$A \equiv \frac{1}{\gamma^2}\left[(\gamma + 1)\alpha\frac{p_4}{p_3} - (\alpha + 1)\right]^2 - (\alpha + 1)^2 + \frac{\gamma + 1}{\gamma^2}(2\gamma\alpha + \gamma - 1)$$

$$B \equiv 2\left[\left\{\frac{(\gamma + 1)p_4\alpha}{\gamma p_3}\right\}^2 - \frac{1}{\gamma}\left\{\frac{(\gamma + 1)p_4\alpha}{\gamma p_3}\right\} \times (2\alpha + 1 + \phi^2\psi) + \frac{1 - \gamma^2}{\gamma^2}(\alpha + 1)(\alpha + \phi^2\psi) + \frac{\gamma + 1}{\gamma^2}\phi\psi(2\gamma\alpha + \gamma - 1)\right]$$

$$C \equiv \frac{1}{\gamma^2}\left[\left\{\frac{(\gamma + 1)p_4\alpha}{p_3} - (\alpha + \phi^2\psi)\right\} - \gamma^2(\alpha + \phi^2\psi)^2 + (\gamma + 1)(2\gamma\alpha + \gamma - 1)\phi^2\psi^2\right]$$

Thus an iterative solution is not necessary for this case.[10]

Appendix B: Tunnel Running Time

The running time t of a tunnel operated with $p_1 = \text{const}$ is given by[22]

$$t = Vp_{r0}\mu/m_3''RT_{r0}[1 - (p_1/p_{r0})^{1/\gamma}]$$

The nozzle mass-flow rate m_3' is given by

$$m_3' = \frac{m_3''}{\mu} = -\frac{Vp_{r0}}{RT_{r0}}\left[\left(\frac{p_R}{p_{r0}^{1/\gamma}}\right)^{(1-\gamma)/\gamma}\frac{1}{\gamma}\frac{dp_R}{dt}\right]$$

thus integration gives, for operation with varying nozzle opening, and varying p,

$$t = -\frac{Vp_{r0}}{m_3''RT_{r0}}\frac{1}{\gamma}\int_1^{p_{Rf}/p_{r0}} \mu\left(\frac{p_1}{p_{r0}}\right)^{(1-\gamma)/\gamma} d\left(\frac{p_1}{p_{r0}}\right)$$

References

[1] Bailey, A. and Wood, S. A., "Development of a High Speed Induced Wind Tunnel," R. & M. 1468, May 1932, Aeronautical Research Council.

[2] Stack, J., "The NACA High Speed Wind Tunnel and Tests of Six Propeller Sections," Rept. 463, 1933, NACA.

[3] Bailey, A. and Wood, S. A., "The Development of a High Speed Induced Wind Tunnel of Rectangular Cross-Section," R & M 1791, Aeronautical Research Council.

[4] Bailey, A. and Wood, S. A., "Further Development of a High Speed Wind Tunnel of Rectangular Cross-Section," R & M 1853, Sept. 1938, Aeronautical Research Council.

[5] Bailey, A. and Wood, S. A., "Conversion of Stanton 3 In. Tunnel," *Proceedings of the Institution of Mechanical Engineers*, Vol. 135, 1937, p. 445.

[6] Knowler, A. E. and Holder, D. W., "The Efficiency of High-Speed Wind Tunnels of the Induction Type," R & M 2448, Aeronautical Research Council.

[7] Poggi, L., "Study of a Type of High Speed Wind Tunnel Working by Ejection with a Steam Jet as the Impelling Fluid," *L'Aerotecnica*, Vol. 19, Nov. & Dec. 1939, British Ministry of Supply.

[8] Lilley, G. M. and Holder, D. W., "Experiments on an Induction Type High Speed Wind Tunnel Driven by Low Pressure Steam," Rept. 24, March 1949, College of Aeronautics, Cranfield, England.

[9] Winter, H., "On the Use of Jet Drives for Wind Tunnels of High Velocity," 1103, Aerodynamische Versuchsanstalt Gottingen e.v., Oct. 1939, Deutsche Luftfahrtforschung Forsehungsbericht; Transl. David Taylor Model Basin, No. 219, 1947.

[10] Keenan, J. H. and Neumann, E. P., "A Simple Air Ejector," *Journal of Applied Mechanics*, Vol. 64, PA-75, June 1942.

[11] Keenan, J. H., Neumann, E. P., and Lustwerk, F., "An Investigation of Ejector Design by Analysis and Experiment," *Journal of Applied Mechanics*, Vol. 17, No. 3, Sept. 1950, p. 299; Vol. 18, No. 1, March 1951, p. 117.

[12] Flugel, G., "The Design of Jet Pumps," March-April 1939, V.D.l. Forshungsheft 395, Transl. NACA TM 982.

[13] Sheldon, J. A. and Huncyak, H. R., "An Analytical and Experimental Evaluation of a Two-Stage Annular Air Ejector for High-Energy Wind Tunnels," TN D 1215, June 1962, NASA.

[14] Neumann, E. P. and Lustwerk, F., "Supersonic Diffusers for Wind Tunnels," *Journal of Applied Mechanics*, Vol. 71, 1949, p. 195.

[15] Reid, E. G., "Annular-Jet Ejectors," TN 1949, 1949, NACA.

[16] Liepmann, H. W. and Puckett, A. E., *Aerodynamics of a Compressible Fluid*, Wiley, New York, 1947, p. 83.

[17] Elrod, H. G., "The Theory of Ejectors," *Journal of Applied Mechanics*, Vol. 12, PA-170, Sept. 1945.

[18] Wattendorf, F. L., "The Efficiency of Return Flow Wind Tunnels," *The Science Reports of National Tsing. Wua. University*, Ser. A, Vol. III, No. 485, July 1936, p. 377.

[19] Wattendorf, F. L., "Energy Ratio of Return Flow Wind Tunnels," *Proceedings of the 5th International Conference of Applied Mechanics*, 1939, p. 526.

[20] Bradshaw, P. and Pankhurst, R. C., "The Design of Low-Speed Wind Tunnels," Aeronautics Rept. 1039, 1962, National Physical Laboratory.

[21] Gibbings, J. C., "The Effects of Varying the Density of the Air in a Model High Speed Tunnel of the Induced Type," Ph.D. thesis, 1951, Univ. of London.

[22] Bidwell, J. M., "Analysis of an Induction Blowdown Supersonic Tunnel," TN 2040, NACA.

[23] Collar, A. R., "Some Experiments with Cascades of Aerofoils," R & M 1768, 1936, Aeronautical Research Council.

[24] Benson, S. F., "Boiler Draught Production by Means of the Jet Air Pump," *Proceedings of the Institution of Mechanical Engineers*, Vol. 153, WEP 9, 1945, p. 31.

[25] Gibbings, J. C., Ingham, J., and Johnson, D., "Flow in a Supersonic Jet Expanding from a Convergent Nozzle," Rept. 30371, Aeronautical Research Council.

[26] Lindsey, W. F., "Choking of a Subsonic Induction Tunnel by the Flow from an Induction Nozzle," TN 2730, July 1952, NACA.

[27] Weatherston, R., "Mixing of any Number of Streams in a Duct of Constant Cross Sectional Area," *Journal of the Aeronautical Sciences*, Vol. 16, No. 11, 1949, p. 697.